

Low-frequency noise in top-gated ambipolar carbon nanotube field effect transistors

Guangyu Xu,^{1,a)} Fei Liu,² Song Han,¹ Kounghmin Ryu,³ Alexander Badmaev,³ Bo Lei,³ Chongwu Zhou,³ and Kang L. Wang¹

¹Department of Electrical Engineering, University of California at Los Angeles, Los Angeles, California 90095, USA

²IBM T. J. Watson Research Center, Yorktown Heights, New York 10598, USA

³Department of Electrical Engineering, University of Southern California, Los Angeles, California 90089, USA

(Received 27 February 2008; accepted 19 May 2008; published online 6 June 2008)

Low-frequency noise of top-gated ambipolar carbon nanotube field effect transistors (CNT-FETs) with aligned CNT growth onto the quartz substrate is presented. The noise of top-gated CNT-FETs in air is lower than that of back-gated devices, and is comparable to that of back-gated devices in vacuum. It shows that molecules in air act as additional scattering sources, which contribute to the noise. Different noise amplitudes in the electron-conduction and the hole-conduction regions are due to different Schottky barriers with respect to the conduction and valance bands as well as the scattering in the channel. © 2008 American Institute of Physics. [DOI: 10.1063/1.2940590]

To date, most of research on carbon nanotube field effect transistors (CNT-FETs) has been focused for their low power consumption and energy delay products.¹⁻⁴ As the device size keeps scaling down, channel scattering and contact properties increasingly impact the device performance. Back-gated CNT-FET structure without passivation has been found to be sensitive to interface defects and/or air molecules.^{5,6} Hence, the reduction of the low-frequency noise level has become an essential issue in realizing CNT-FET for practice use. Top-gated FET structure is a natural choice for realistic electronic systems. The Al₂O₃ gate dielectric acting as a passivation layer to the *p*-type CNT-FETs has been shown to stabilize their electrical characteristics, and to lower the noise of the drain-to-source CNT resistance on a Si/SiO₂ substrate without gate bias.⁷ However, the CNT synthesis on the Si/SiO₂ substrate normally cannot control the CNT growth direction and the device structure has large parasitic capacitances, which limits their use for manufacturable CNT integrated circuits.⁸

Recently reported high performance devices were realized by using aligned CNT growth on the quartz substrate.^{8,9} With the aligned CNT in a controllable direction, it is possible to reduce the crossover and misalignment among CNTs. Investigations on noise performance of this top-gated structure device will be helpful in designing CNT-FETs with a good signal to noise ratio for potential device and circuit integrations. In this work, the noise power spectrum density (PSD) was measured using Agilent 35670A after the signal was passed through a low noise operational amplifier; a Keithley 4200 was used for device characterization under bias.

Top-gated CNT-FETs reported here were fabricated onto a 500 μm thick quartz substrate shown in the inset of Fig. 1(a). The aligned growth of single-walled CNTs was achieved using a chemical vapor deposition method.⁸ The source/drain contacts of different widths were made by deposition of Ti/Au metal films (3/50 nm). The carrier transport of the devices was believed to be within the diffusive limit

since the channel length was as long as 4 μm.¹⁰ The density of CNTs was roughly 4 CNTs/μm of the channel width, with the diameters varying from 1 to 2 nm as observed in the scanning electron micrograph (SEM) inset. A 24 nm HfO₂ gate oxide was deposited by atomic layer deposition, followed by depositing a 2 μm Au gate electrode defined by ebeam writing in the middle between the source and drain.

Figure 1(a) also shows the typical ambipolar transfer characteristics of a top-gated CNT-FET. Since both metallic and semiconducting CNT channels were present, a burning process was used to remove metallic ones. In the burning process, V_{ds} was increased in order to burn metallic CNT

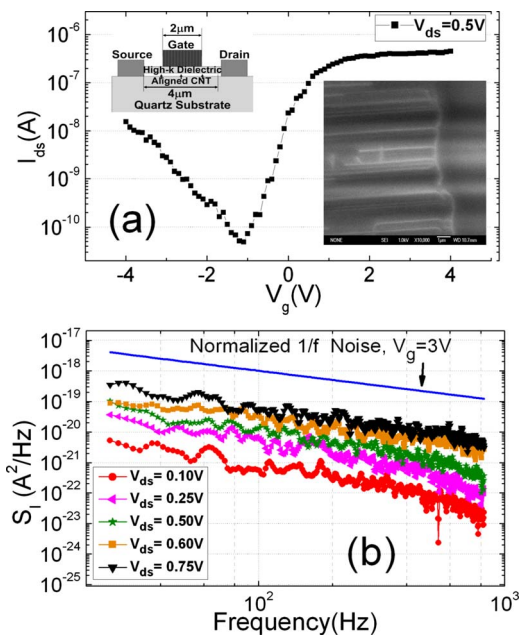


FIG. 1. (Color online) (a) Typical ambipolar transfer characteristics of top-gated CNT-FET with $V_{ds}=0.5$ V at room temperature. Inset: the schematic of the device and the SEM picture of the aligned CNTs (bright lines) grown on the quartz substrate. (b) Typical noise PSD in air under room temperature at $V_g=3$ V vs V_{ds} , showing a typical $1/f$ behavior. The solid line shows the normalized $1/f$ noise scaled to $S_I=10^{-18}$ A²/Hz at $f=100$ Hz.

^{a)}Electronic mail: guangyu@ee.ucla.edu.

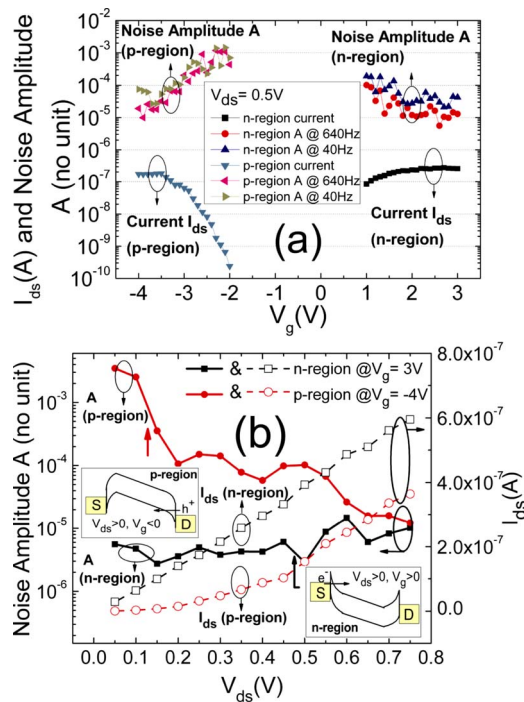


FIG. 2. (Color online) (a) Noise amplitudes (A) and current (I_{ds}) under different gate biases near $f=40$ and 640 Hz in both the electron-conducting (n) and the hole-conducting (p) regions. Transfer characteristics (I_{ds} - V_g) for both regions are plotted in the same scale on the left. The noise amplitudes for both regions are inversely related to the drain current. (b) Noise amplitudes (A) under different source-drain biases for $f=640$ Hz for both regions (on the left scale). I_{ds} - V_{ds} curves are also shown with V_{ds} ranging from 0.05 to 0.75 V (on the right scale). Inset: a different trend of the noise dependence on V_{ds} is attributed to SBs with respect to the conduction band (n -region) and valance band (p -region).

channels. After the burning process, the I_{on}/I_{off} current ratio was improved.⁹ I_{on} was typically observed to change from $1-10 \mu A$ to $0.001-0.1 \mu A$ before and after the burning process, respectively. However, the effective CNT density was reduced. Experiments were done for six CNT-FET devices but all the data shown in this paper came from the same device. In testing, five out of six devices show ambipolar characteristics while one device shows only p -type characteristics with the applied gate bias typically ranging from -4 to 4 V. The gate leakage current was generally observed in the range of $0.1-1$ pA.

Figure 1(b) shows typical room temperature noise PSD for the frequency range from 25 to 800 Hz for $V_g=3$ V (n -region), and V_{ds} varying from 0.10 to 0.75 V. Measurements were made in air. A hysteresis effect (a threshold shift is less than 1 V) was observed. Noise data after subtracting the background were collected by a similar method as before.¹⁰ The low-frequency noise shows $1/f^\alpha$ behavior for the frequency range from 0.125 Hz to 25.6 kHz (not shown) with α ranging from 1.02 to 1.23 . The deviation of the $1/f$ shape is probably due to other noise mechanisms such as a random telegraph signal from an individual scattering trap, which has a Lorentzian noise characteristic of its own.¹¹

The noise amplitude A is defined as $A=S_f(f/I^2)$ since all devices show typical $1/f$ noise behavior in both n and p regions. Figure 2(a) shows part of the I_{ds} - V_g relationship for the ambipolar device at $V_{ds}=0.5$ V, where the currents were collected at the same time with the noise. The noise amplitude data (A) approximately at $f=40$ Hz and $f=640$ Hz for both regions are shown to be inversely related to the drain

current I_{ds} . This trend is similar to those reported in wide ranges of nanotube conductors, where the noise amplitude is inversely related to the sample conductance.¹² For the p -region with V_g ranging from -4 to -2 V, A and I_{ds} show two and three orders of change, respectively, which is consistent with four orders of change of the total noise level (S_I) (not shown). For the n -region with V_g ranging from 1 to 3 V, the variation of noise amplitude (A) with V_g are smoother than those in the p -region since both I_{ds} and S_I change less than one-order. In general, while it is still not clear about the gate dependence to the noise performance for certain CNT-FET structures, it is observed here that as the gate bias is biased to the subthreshold regime, the noise amplitude A becomes larger. It may be due to a smaller sample conductance when the device operates closer to the subthreshold regime, where a higher relative current fluctuations ($\Delta I_{ds}/I_{ds}$) from both the channel scattering and Schottky barrier (SB) contact transmission coefficient happen.⁵

Figure 2(b) shows the dependence of the noise amplitude to the source-drain bias, V_{ds} , for the n -region ($V_g=3$ V) and the p -region ($V_g=-4$ V), respectively (shown in the inset). The I_{ds} - V_{ds} curve at $V_g=3$ V is shown to be linear, indicating that the contact is almost Ohmic due to a small SB width to the conduction band for electron conduction. On the other hand, the I_{ds} - V_{ds} curve at $V_g=-4$ V shows a typical SB characteristics, which is due to the larger SB width to the valence band for the hole conduction. The noise amplitude for $f=640$ Hz is presented. For the n -region at $V_g=3$ V, the noise amplitude is generally less than 2×10^{-5} , roughly in the same order of amplitude with increasing I_{ds} , similar to back-gated devices biased in the linear region.¹⁰ For the p -region at $V_g=-4$ V, the noise amplitude decreases from 10^{-3} to 10^{-5} with increasing I_{ds} while approaching the same order as the n -region at $V_g=3$ V. This is due to the decreasing SB contact resistance with an increasing V_{ds} for the p -region, lowering the corresponding noise amplitude. From an earlier work,⁶ this noise amplitude is also attributed to the channel scattering, which causes the current fluctuation in the device. It is noted that the sample conductance increases with V_{ds} for the p -region ($V_g=-4$ V), where the transmission coefficient of the SB contact is approaching to be near unity. Hence the noise is almost all due to the channel scattering, and is in the same order of magnitude for both regions, as seen in Fig. 2(b) for large V_{ds} . The different trend of the noise dependence on V_{ds} for both regions is most likely due to different SB widths with respect to the conduction band and valance band.

For comparison of noise levels for different CNT-FET devices, Fig. 3 shows the $A-R_{ds}$ for the devices of this work along with those reported in previous references.^{5,6,10,12,13} The detailed descriptions of CNT-FET structures in comparison are listed in Table I.¹⁴ In the linear I_{ds} - V_{ds} regime, the sample resistance R_{ds} is defined as V_{ds}/I_{ds} . Typical points are picked from the published data and our measurements from all six devices. The noise amplitude in the top-gated CNT-FETs of this work in air is shown to be lower compared to that of the back-gated devices in air, while roughly the same as that of the back-gated devices in vacuum. It suggests that molecules in air act as additional scattering sources to contribute to the noises. The HfO₂ high- k top-gated CNT-FETs in this work shows one to two orders of amplitude lower in the noise amplitude (A) than a reported p -type Al₂O₃ high- k

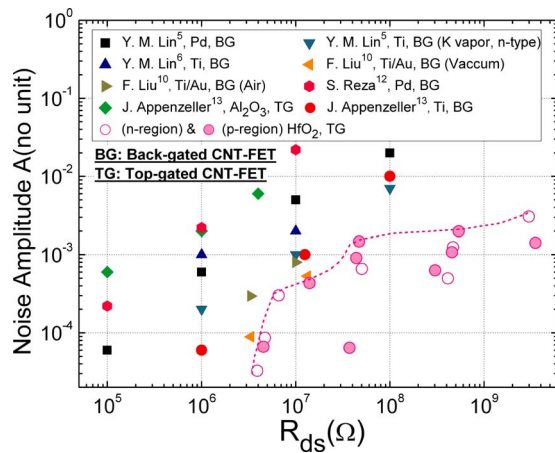


FIG. 3. (Color online) Noise amplitude of this work (below the dashed line) and other previous works (Refs. 5, 6, 10, 12, and 13). The $A-R_{ds}$ relationships are plotted with the sample resistance R_{ds} ranging from 10^5 to 10^{10} Ω . Typical points are picked from the published data and our measurements for six devices in the linear region (the deviation of linearity is smaller than 10%). The noise amplitude in the devices of this work in air is shown to be lower compared to that of the back-gated devices in air, while it is roughly the same as that of the back-gated devices in vacuum.

top-gated device near $R_{ds}=4 \times 10^6$ Ω , which might be due to better high- k dielectric quality, the improved contact properties, and the large channel length¹³ (see a later discussion). The noise amplitude generally increases with R_{ds} , which is similar to reported CNT devices.¹⁵ Our devices have a one to two orders of magnitude lower sample conductance than previous work,^{5,10} which may be due to the burning process and small gate biases.

The impact of channel length to the noise amplitude is qualitatively discussed below. Table I shows the noise amplitudes of different CNT-FETs near $R_{ds}=10^7$ Ω , with the channel length (l) ranging from 600 nm to 4 μm . The R_{ds} of CNT-FETs is generally expressed as $R_{ds}=R_{SB}+(h/4e^2)(l/\lambda)$, where R_{SB} is the contact resistance and λ is the electron mean free path.⁵ Hence, R_{ds} with decreasing channel length should become more contact dominated. It is known that R_{SB} is generally sensitive to both the electric field at the contact

TABLE I. Details of CNT-FETs listed in Fig. 3. The noise amplitude (A) from different pieces of work is shown for $R_{ds} \approx 10^7$ Ω for comparison. BG and TG stand for back-gated and top-gated CNT-FETs, respectively.

Data source	Contact	Structure	L_{channel}	Exposure	A ($R_{ds} \approx 10^7$ Ω)
Lin et al. ^a	Pd	BG	600 nm	Air	5×10^{-3}
Lin et al. ^a	Ti	BG	300 nm	K vapor	1×10^{-3}
Lin et al. ^b	Ti	BG	600 nm	Air	2×10^{-3}
Liu et al. ^c	Ti/Au	BG	4 μm	Air	8×10^{-4}
Liu et al. ^c	Ti/Au	BG	4 μm	Vacuum	5.33×10^{-4}
Reza et al. ^d	Pd	BG	1 μm	Air	2.2×10^{-2}
Appenzeller et al. ^e	Pd	TG (Al_2O_3)	200 nm	Air	6×10^{-3}
Appenzeller et al. ^e	Ti	BG	600 nm	Air	1×10^{-3}
Here	Ti/Au	TG (HfO_2)	4 μm	Air	4.33×10^{-4}

^aReference 5.

^bReference 6.

^cReference 10.

^dReference 12.

^eReference 13.

and the adsorbed gases.¹⁶ Hence, the noise of those devices with a shorter channel length will be more related to the contact geometry and the exposure in air, which will in turn, significantly impacts R_{SB} . Through the comparison, however, it is noted that the noise amplitude may also be determined by other factors which alter the sample conductance such as scattering due to air molecules, the CNT-oxide interface quality and other contact properties. For example, it is shown that the back-gated device in Ref. 10 has the same channel length ($l=4$ μm) and contact material (Ti/Au) with a similar HfO_2 top-gated FET reported here, while the top-gated devices still show a smaller noise amplitude than the back-gated devices because of the high- k dielectric passivation. In addition, the Pd contacted back-gated device in Ref. 12 has a longer channel length ($l=1$ μm) than Ti contacted back-gated devices in Ref. 13 ($l=600$ nm), while the Pd contacted devices have a much higher noise amplitude due to the contact properties. Hence, a comprehensive study of the device dimension, contact engineering and the channel passivation is needed for low noise CNT-FET designs.

In summary, the low-frequency noise level of top-gated CNT-FETs was shown to be lower compared to those of back-gated devices in air, and roughly the same as that of back-gated devices in vacuum. This result shows that attached molecules in air act as the additional scattering sources of the noise. Different noise behaviors in both n and p regions were due to different SBs with respect to the conduction band and valance band as well as the channel scattering. This device offers a low noise CNT-FET structure with potentially high on currents.

We acknowledge experimental help from X. Han and M. Bao. This work was in part supported by MARCO Focus Center on Functional Engineered Nano Architectonics (FENA), monitored by Dr. Betsy Weitzman.

¹A. Javey, J. Guo, Q. Wang, M. Lundstrom, and H. J. Dai, *Nature (London)* **424**, 654 (2003).

²J. Kong, N. R. Franklin, C. Zhou, M. G. Chapline, S. Peng, K. Cho, and H. Dai, *Science* **287**, 622 (2000).

³P. G. Collins, K. Bradley, M. Ishigami, and A. Zettl, *Science* **287**, 1801 (2000).

⁴S.-H. Hur, O. O. Park, and J. A. Rogers, *Appl. Phys. Lett.* **86**, 243502 (2005).

⁵Y. M. Lin, J. Appenzeller, J. Knoch, Z. H. Chen, and Ph. Avouris, *Nano Lett.* **6**, 930 (2006).

⁶Y. M. Lin, J. Appenzeller, Z. H. Chen, and Ph. Avouris, *Physica E (Amsterdam)* **37**, 72 (2007).

⁷S. K. Kim, Y. Xuan, P. D. Ye, S. Mohammadi, J. H. Back, and M. Shim, *Appl. Phys. Lett.* **90**, 163108 (2007).

⁸X. L. Liu, S. Han, and C. W. Zhou, *Nano Lett.* **6**, 34 (2006).

⁹S. J. Kang, C. Cocabas, T. Ozel, M. Shim, N. Pimparcar, M. A. Alam S. V. Rotkin, and J. A. Rogers, *Nat. Nanotechnol.* **2**, 230 (2007).

¹⁰F. Liu, K. L. Wang, D. H. Zhang, and C. W. Zhou, *Appl. Phys. Lett.* **89**, 063116 (2006).

¹¹A. P. van der Wel, E. A. M. Klumperink, L. K. J. Vandamme, and B. Nauta, *IEEE Trans. Electron Devices* **50**, 1378 (2003).

¹²S. Reza, Q. T. Huynh, G. Bosman, J. Sippel-Oakley, and A. G. Rinzler, *J. Appl. Phys.* **100**, 094318 (2006).

¹³J. Appenzeller, Y. M. Lin, J. Knoch, Z. H. Chen, and Ph. Avouris, *IEEE Trans. Nanotechnol.* **6**, 3 (2007).

¹⁴The data from Ref. 12 is calculated by the lowest averaging A/R_{ds} value for the semiconducting CNTs.

¹⁵P. G. Collins, M. S. Fuhrer, and A. Zettl, *Appl. Phys. Lett.* **76**, 894 (2000).

¹⁶S. Heinze, J. Tersoff, R. Martal, V. Derycke, J. Appenzeller, and Ph. Avouris, *Phys. Rev. Lett.* **89**, 106801 (2002).